Effect of rotor induction on the propagation of disturbances towards wind turbines

Authors

A. Abdelsalam[2], K. Boorsma[1], F. Savenije[1], M. Boquet[2], S. Davoust[2], R. Rutteman[3]

Corresponding author: boorsma@ecn.nl

www.ecn.nl
P.O. Box 1
1755 ZG Petten
The Netherlands

Introduction

Within the framework of the LAWINE project (LiDAR Applications for Wind Farm Efficiency), the application of LiDAR for optimization of turbine control is researched. The evolution of turbulent structures as they approach a wind turbine is critical in order to link turbine loads to free-stream turbulence with special attention given to Taylor's hypothesis of frozen turbulence. Secondly, knowing the coherency and timing for the arrival of such structures is required for future use of LiDAR for feed-forward control.

In the present work, a 5 beam pulsed LiDAR has been mounted on turbine to characterize rotor induction and its effects on the propagation of disturbances towards wind turbines.

Test set-up

The ECN EWTW test site in Wieringermeer, The Netherlands is used for the test campaign. A 5 MW XEMC Darwind turbine has been equipped with a 5-beam Demonstrator Avent LiDAR. This LiDAR is a demonstrator instrument specifically designed for turbine control research & development projects. Pictures of both the turbine and LiDAR are given below.

Characterisation of the induction effect

The induction is calculated using the formula below. The induction parameter $a = 1 - V/V_\infty$ is found using a least square fit to the experimental data using the central beam. The results agree with the generally expected variation of rotor induction throughout the operational regime.

$$\frac{V(\zeta)}{V_\infty} = 1 - a\left[1 + \zeta(1+\zeta^2)^{-1/2}\right]$$

$$\zeta = x / R$$

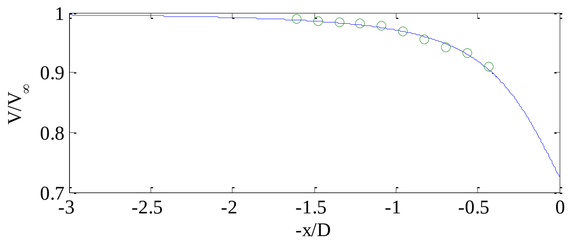

Fig. 1 Free-stream velocity as a function of the distance from the rotor (circles),together with fitted wind model to determine the induction parameter.

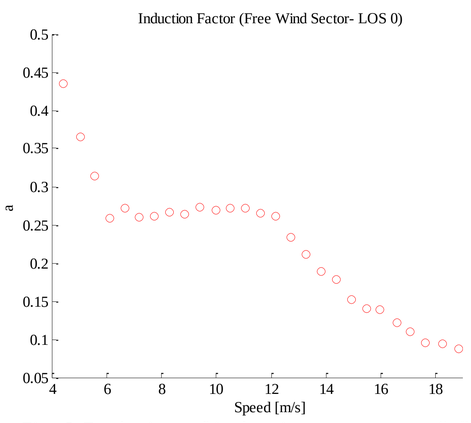

Fig. 2 Evolution of induction parameter "a" as a function of free-stream wind speed.

Turbulence Evolution

The evolution of turbulence intensity as the flow approaches the rotor is studied for different free-stream velocities using the central beam.

- The turbulence intensity (normalised by the local averaged wind speed) shows a gradual increase whilst approaching the rotor (Fig 3). The velocity fluctuations are constant with distance to the rotor (Fig 4) , which leads to the increase of turbulent intensity,.
- The high wind speeds do show a slight increase of the turbulent fluctuations when approaching the rotor (Fig 4).

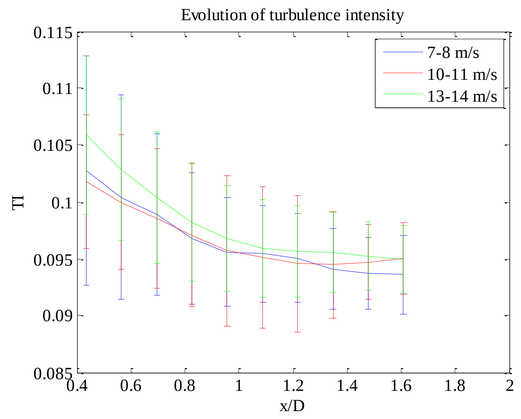

Fig. 3 Evolution of turbulence intensity as a function of normalized axial distance for various free-stream velocities for $0.09 \le TI \le 0.10$

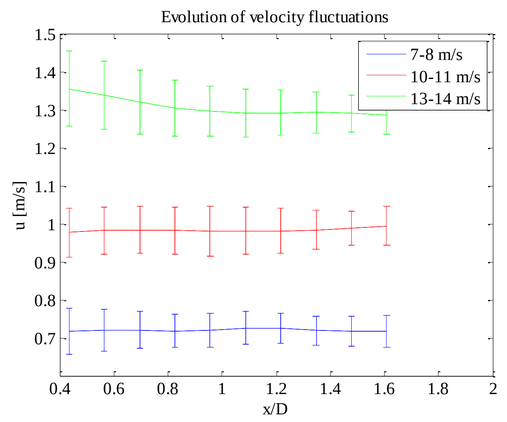

Fig. 4 Evolution of velocity fluctuations u' as a function of normalized axial distance for various free-stream velocities for $0.09 \le TI \le 0.10$

Turbulent convective speed

The convective speeds are calculated using three different approaches: Integration of the blockage model with respect to axial distance, effectively giving Taylor's convective wind speed, cross correlations and phase spectrum.

- Cross correlations and phase spectrum provide slightly higher estimates than the blockage model with both showing a sudden drop for high wind speeds (Fig 5).
- The phase spectrum shows that for high wind speeds there is a clear separation in the convective speeds of the different turbulent structures sizes (Fig 6). Low data availability at these velocities and numerical implementation could be the reason for the difference.

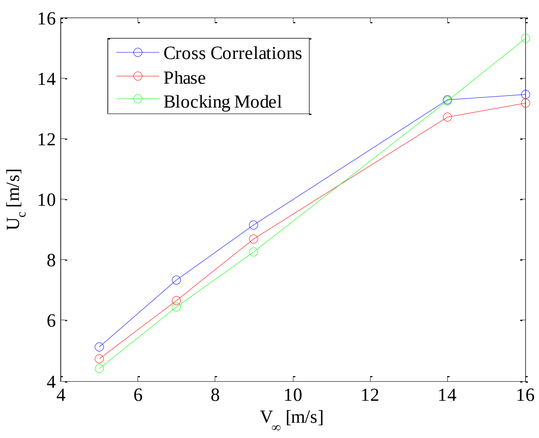

Fig. 5 Comparison of the various methods utilized to estimate the convective velocities U_c

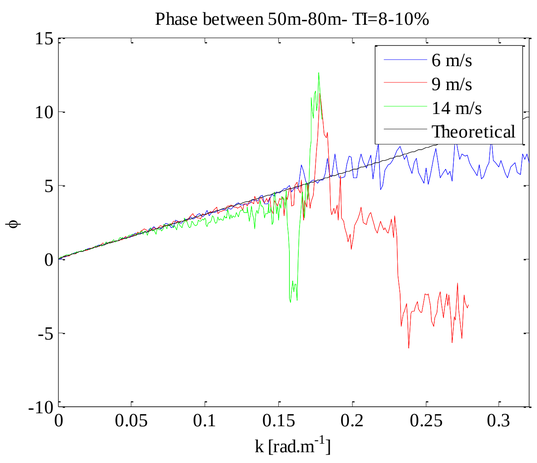

Fig. 6 Phase spectrum of measurements taken at two upstream location for various free stream wind speeds as a function of wavenumber $k = 2\pi / Vt$

Conclusion

A successful test campaign with a 5-beam Demonstrator Avent LiDAR has been performed. A first analysis of the data shows:

- The evolution of turbulence shows an increase in intensity approaching the rotor mainly due to decrease of the average wind speed and constant turbulent fluctuations (high wind speeds excepted).
- The convective speed of the turbulent structures seems to depend on the size of the structures unlike Taylor's hypothesis suggests. This would seem to be more pronounced for high wind speeds which would explain the sudden drop in the estimates for high wind speeds using both spatial-temporal and spectral methods.

Acknowledgements

TKI WIND OP ZEE

Partners

ECN
avent Lidar Technology
TU Delft
XEMC DARWIND sea-change in wind energy

[1] ECN Wind Energy, P.O. Box 1, 1755 ZG Petten, The Netherlands

[2] Avent Lidar Technology, Orsay, France

[3] XEMC Darwind, Hilversum, The Netherlands

Effects of rotor induction on the propagation of disturbances towards wind turbines

A. Abdelsalam*, K. Boorsma, F.J. Savenije, S. Davoust*, R. Rutteman+

ECN Wind Energy, P.O. Box 1, NL 1755 ZG Petten, the Netherlands
* Avent Lidar Technology, Orsay, France
+ XEMC Darwind, Hilversum, the Netherlands

Summary

In the present study the induction upstream of a 5 MW wind turbine is characterised using a mathematical model and validated against experimental data obtained with a nacelle mounted multi-beam LiDAR from Avent Lidar Technology. The convective speed of turbulent structures are computed using spatial-temporal and spectral methods and compared with that of the mathematical model describing the slowing down of the flow. For different wind speeds, longitudinal wind speed variance stayed constant with the distance to the rotor while the observed turbulence intensity increased due mainly to the decrease of longitudinal mean wind speed. The spatial-temporal methods provide higher convective speed estimates than the spectral methods while both estimated speeds appear to follow linearly the free stream wind speed but with a deviation for high wind speeds. Higher turbulent frequencies seem to be convected at higher speeds.

1. Introduction

1.1 Background

Within the framework of the LAWINE project (LiDAR Applications for Wind Farm Efficiency), the application of LiDAR for optimization of turbine control is researched. The evolution of turbulent structures as they approach a wind turbine is critical in order to link turbine loads to free-stream turbulence. Secondly, knowing the coherency and timing for the arrival of such structures is required for future use of LiDAR for feed-forward control [1]. According to Taylor [6], for low turbulence levels, turbulent structures are convected by a large mean flow in a time shorter than the evolution time of the eddies, and could therefore be considered frozen. The validity of this hypothesis will be tested to find out to what extent it holds and if convection speed depends on turbulent scale.

Fig. 1 Avent's five-beam LiDAR

In the present work, a 5-beam Demonstrator Avent LiDAR has been mounted on a turbine to characterize the rotor induction and its effects on the propagation of disturbances towards wind turbines. This LiDAR is a demonstrator instrument specifically designed for turbine control research & development projects

1.2 Test set-up and data analysis

The analysis of experimental data presented in this report stems from a 7 month campaign ran at the Energy research Center of the Netherlands (ECN), where a 5 beam LiDAR from Avent, Figure 1, was installed on an industrial multi-megawatt wind turbine. The site is composed of flat terrain located near the shore, and the average annual wind speed at a 100m height above the ground is 11.5m/s with a turbulence intensity ranging from 5% to 20%.

The wind turbine in question is a 5MW, 115m diameter wind turbine, with a 12 m/s nominal wind speed. The LiDAR beams are configured in a "plus" configuration as depicted by Figure 2. With its 4 Hz refresh rate it fires beams with a 15° cone half angle with 10 measurement gates from 50m to 185m.

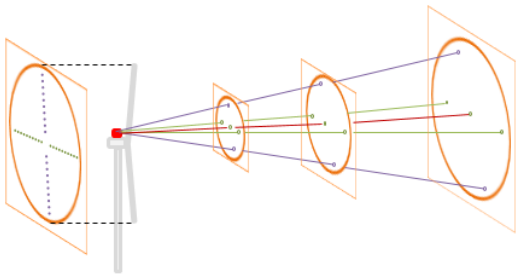

Fig. 2 LiDAR beam configuration.

A standardised 10 minutes duration is used to compute averages and statistics. Due to the large amount of data gathered over the campaign some filters had to be applied, namely on the minimum rotational speed, free stream wind speed and wind sector. For the present paper, the experimental data from the central beam has been used.

2. Methods

2.1 Characterisation of the induction effect

The induction effect, also known as the blockage effect, is the result of the wind being slowed down by the obstacle that is the wind turbine. The blockage effect has been thoroughly investigated numerically [2][3] as well as experimentally in controlled laboratory environment. However it has only been lightly studied at full scale with a LiDAR, mostly because it is very difficult measuring velocities everywhere in a plane in front of the rotor. This induction effect is characterized using the actuator disk theory by a non-dimensional coefficient $a = 1 - V/V_\infty$, where V is the velocity on the rotor at hub height and V_∞ the free stream velocity. This theory also expresses the power coefficient in terms of the induction coefficient, as:

$$C_P = 4a(1-a)^2 \quad (1)$$

The maximum power coefficient is then theoretically obtained for a value of $a = 1/3$ [4]. Using the Biot-Savart law to the vortex filament shed by the blade tips and moving in a helical fashion, is possible to obtain an expression for the axial variation the induced velocity upstream the rotor plane as follows [5]:

$$\frac{V(\zeta)}{V_\infty} = 1 - a\left[1 + \zeta(1+\zeta^2)^{-1/2}\right] \quad (2)$$

where $\zeta = x/R$, is the axial distance normalized by the radius of the rotor. Figure 3 shows a fit of (2) on experimental data gathered over 10 minutes by the LiDAR's central beam that is perfectly aligned with the turbine axis. In that particular case an induction factor $a = 0.25$ fits best the experimental data.

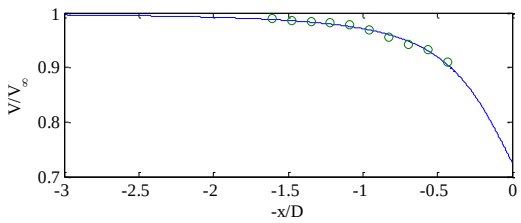

Fig. 3 Free-stream velocity as a function of the distance from the rotor (circles), together with fitted wind model to determine the induction parameter.

Using a least square fitting method the induction parameter can be computed for various free-stream wind speeds, as shown in Figure 4. Three regions are visible, one being of a constant induction parameter corresponding to the optimal operating state of the wind turbine, seen here to be roughly 0.27. The results agree with the generally expected variation of rotor induction throughout the operational regime.

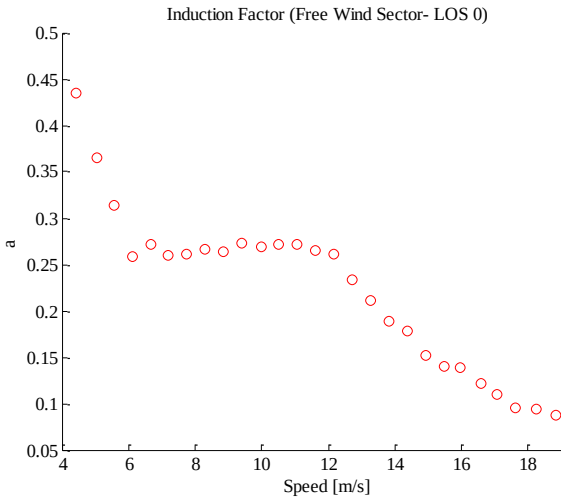

Fig. 4 Evolution of induction parameter "a" as a function of free-stream wind speed.

2.2 Cross-correlations

Any given flow can be decomposed into an average and fluctuating component, $u = \langle u \rangle + u'$. The turbulence intensity is then $u'/\langle u \rangle$, which is simply put the standard deviation of the wind speed time history, taken by default over a 10 minute period. To first estimate the convective velocity, cross-correlations are computed between 50 meters upstream of the rotor; and all other measuring distances, using

$$R_{ij}(\tau) = \left\langle x_i(t) x_j(t+\tau) \right\rangle \quad (3)$$

$$\rho_{ij}(\tau) = \frac{R_{ij}}{\sigma_{ii}(0)\sigma_{jj}(0)} \quad (4)$$

The cross correlation normalized by the auto-covariance leads to a more useful quantity, the cross-correlation coefficient (4). The maximum cross correlation coefficient for the various separation distances, leads to a given time lag τ from which the convective speed is calculated. Fig 5 shows the plot of the measurement separation distance as a function of this time lag, whose slope is in theory the convective velocity. Data points used for this plot were selected to be at $9\ m/s \pm 0.2$.

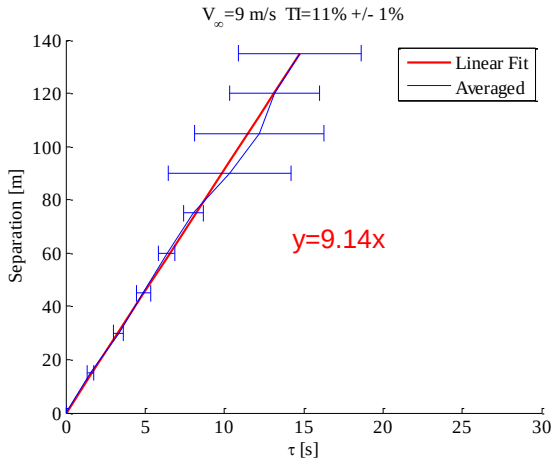

Fig. 5 Correlation distance as a function of time lag corresponding to maximum correlation.

2.3 Spectral analysis

The second method used to estimate the convective speeds consisted of computing the magnitude squared coherence:

$$\gamma^2(f) = \frac{\left|\left\langle E_{ij}(f)\right\rangle\right|^2}{\left\langle E_{ii}(f)\right\rangle\left\langle E_{jj}(f)\right\rangle} \quad (5)$$

Where

$$E_{ij}(f) = \int_{-\infty}^{+\infty} R_{ij} e^{-i2\pi f\tau} dt \quad (6)$$

and then computing the phase, which carries the velocity information. A constant convective speed across all turbulent structures should in fact yield a linear relationship between the phase (7) and the frequency.

$$\theta(f) = \arctan\left(\frac{\mathrm{Im}\left\{\left\langle E_{ij}(f)\right\rangle\right\}}{\mathrm{Re}\left\{\left\langle E_{ij}(f)\right\rangle\right\}}\right) \quad (7)$$

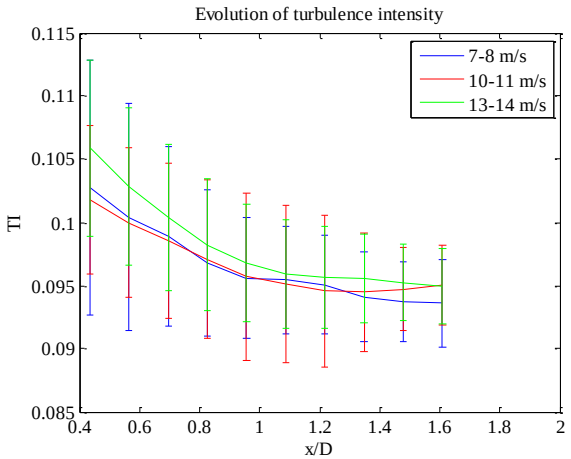

Fig. 6 Evolution of turbulence intensity as a function of normalized axial distance for various free-stream velocities for $0.09 \le TI \le 0.10$.

3. Results and discussions

3.1 Turbulence evolution

The evolution of the turbulence intensity as the flow approaches the rotor, for different free-stream velocities, is shown in Figure 6. The data were filtered to have a free-stream turbulence intensity between 9% and 10%. As Figure 6 shows, the turbulence intensity is increasing as it approaches the rotor. As a matter of fact, at first order the velocity fluctuations are constant upstream of the rotor while the mean flow is slowed down, Figure 7. The fact that the longitudinal fluctuations do not significantly evolve as the flow approaches the rotor suggests that the strength of the deceleration is not sufficient to alter the structure of the turbulence. In fact the fluctuations are practically not affected by the induction zone. This however does not seem to hold true for all velocities as the fluctuations in the 13-14 m/s range show an increase in the vicinity of the rotor, Figure 7.

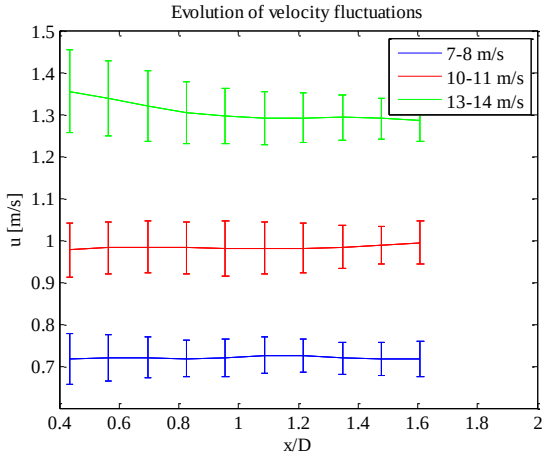

Fig. 7 Evolution of velocity fluctuations u' as a function of normalized axial distance for various free-stream velocities for $0.09 \le TI \le 0.10$

3.2 Convective velocity

The convective velocities were calculated using three different approaches. The first one consisted of integrating the induction model (2) with respect to axial distance. This method gives the mean wind speed as a function of axial position thus the convective wind speed with respect to Taylor's hypothesis.The second method consisted of computing the lag associated with the maximum cross correlation between the measurements at x/D=0.46 and the other measurement gates. The third method consisted of computing the phase of the magnitude squared coherence. The results obtained with all three methods are plotted for different free-stream velocities in Fig 8.

The convective speeds computed by the cross correlation method provides the highest estimates among all three followed by the spectral method. Cross correlations take into account all turbulent scales while spectral methods differentiates between all of them thus giving more pertinent estimates with regard to the dependence on the eddy size.

In both cases there is a sudden drop for wind speeds greater than 14 m/s, as if it were affected by the induction zone. This is in apparent contradiction with the fact that the induction effect is decreasing for high wind speeds as shown in Figure 4. It would seem that for these speeds, smaller eddies travel faster than the big ones. Figure 9 shows the phase as function of wavenumber for the various wind speed ranges, and a clear deviation from the theoretical curve, that of constant convective speed, is apparent for high wind speed. Due to the LiDAR frequency limitations, further information on these small eddies cannot be obtained.

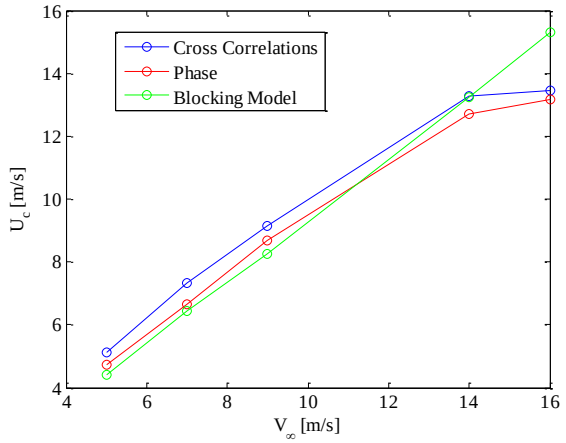

Fig. 8 Comparison of the various methods utilized to estimate the convective velocities U_c.

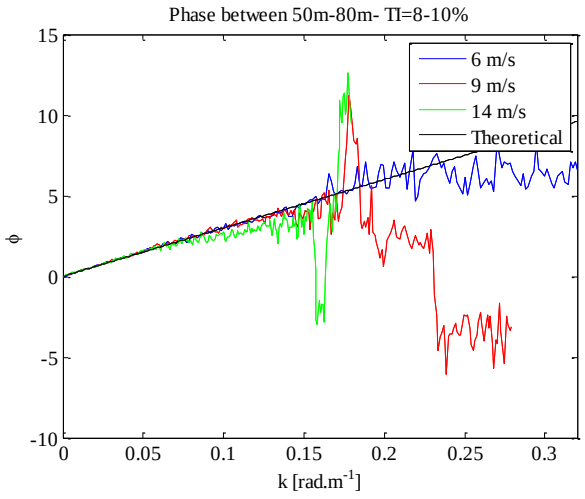

Fig. 9 Phase angle, in radians,of measurements taken at two upstream location for various free stream wind speeds, as a function of wavenumber $k = 2\pi / Vt$.

4.Conclusions

The induction zone was characterized using a 5-beam Demonstrator Avent LiDAR mounted on a 5 MW XEMC Darwind turbine. The evolution of the velocity upstream of the rotor fitted on first order a mathematical model derived from actuator disk theory and vortex theory by Johnson [5]. The induction parameters computed with this model were in line with what the theory predicted for the optimal operating conditions.

The evolution of the turbulence showed an increase in turbulence intensity in the vicinity of the rotor. This was explained by the fact that the velocity fluctuations were not affected by the induction effect and stayed constant as they approached the rotor, while the mean flow decelerated. This is however not a generality as for high wind speeds, an increase in velocity fluctuations was observed.

The estimations of the turbulent structures convective speed showed few discrepancies between all three methods used. Cross correlations provided higher estimates than spectral methods with both showing a linear variation with respect to free stream wind speed and sudden drop for high wind speeds. It was concluded that different turbulent scales travel at different speeds and therefore spectral methods were best suited for this task. Simply taking into account the average wind speed as suggested by Taylor's hypothesis provides lower estimates primarily due the lack of separation of turbulent scales. It is recommended to further study the present data set and investigate the cause for the observed differences at high wind speeds

5. References

[1] Importance of lidar measurement timing accuracy for wind turbine control.Dunne, F., Pao, L.Y., Schlipf, D., Scholbrock, A.K. (ACC), 2014.

[2] Medici, D., Dahlberg, J. and Alfredsson, P. (2009). Measurements of the Flow Upstream a Rotating Wind Turbine Model. Springer, pp.87--90.

[3] Simley, E., Pao, L., Gebraad, P. and Churchfield, M., (2014). Investigation of the Impact of the Upstream Induction Zone on LIDAR Measurement Accuracy for Wind Turbine Control Applications using Large-Eddy Simulation. Journal of Physics: Conference Series 524(1), p.012003.

[4] Burton, Tony. Wind Energy. Chichester: J. Wiley, 2011.

[5] Johnson, W. (1980). Helicopter theory. 1st ed. Princeton, N.J.: Univ. Pr.

[6] G. I. Taylor, "The spectrum of turbulence," in Proc. Royal Society of London, Series A, Mathematical and Physical Sciences, vol. 164, no. 919, 1938, pp. 476–490

Acknowledgement

The work has been performed within the framework of the LAWINE project, sponsored by TKI Wind op Zee.